Baryon Stopping in Heavy-Ion Collisions at $E_{\rm lab} = 2$–160 GeV/nucleon

Yu.B. Ivanov[1, 2, *]

[1] *GSI Helmholtzzentrum für Schwerionenforschung GmbH, D-64291 Darmstadt, Germany*
[2] *Kurchatov Institute, Moscow RU-123182, Russia*

It is argued that the experimentally observed baryon stopping may indicate (within the present experimental uncertainties) a non-monotonous behaviour as a function of the incident energy of colliding nuclei. This can be quantified by a midrapidity reduced curvature of the net-proton rapidity spectrum. The above non-monotonous behaviour reveals itself as a "zig-zag" irregularity in the excitation function of this curvature. The three-fluid dynamic calculations with a hadronic equation of state (EoS) fail to reproduce this irregularity. At the same time, the same calculations with an EoS involving a first-order phase transition into the quark-gluon phase do reproduce this "zig-zag" behaviour, however only qualitatively.

PACS numbers: 24.10.Nz, 25.75.-q
Keywords: relativistic heavy-ion collisions, baryon stopping, hydrodynamics, phase transition

I. INTRODUCTION

A degree of stopping of colliding nuclei is one of the basic characteristics of the collision dynamics, which determines a part of the incident energy of colliding nuclei deposited into produced fireball and hence into production of secondary particles. The deposited energy in its turn determines the nature (hadronic or quark-gluonic) of the produced fireball and thereby its subsequent evolution. Therefore, a proper reproduction of the baryon stopping is of prime importance for theoretical understanding of the dynamics of the nuclear collisions.

A direct measure of the baryon stopping is the net-baryon rapidity distribution. However, since experimental information on neutrons is unavailable, we have to rely on proton data. Presently there exist extensive experimental data on proton (or net-proton) rapidity spectra at AGS [1–4] and SPS [5–9] energies. These data were analyzed within various models [10–18] The most extensive analysis has been done in [14, 17]. Since that time new data at SPS energies have appeared [7–9]. Therefore, it is appropriate to repeat this analysis of already extended data set. In the present Letter it is done within the framework of the model of the three-fluid dynamics (3FD) [17].

II. ANALYSIS OF EXPERIMENTAL DATA

Available data on the proton (at AGS energies) and net-proton (at SPS energies) rapidity distributions from central heavy-ion collisions are presented in Fig. 1. Only the midrapidity region is displayed in Fig. 1, since it is of prime interest in the present consideration. The data at $10A$ GeV are repeated in the right panel of Fig. 1 in order to keep the reference spectrum shape for the comparison. The data are plotted as functions of a "dimensionless" rapidity $(y - y_{cm})/y_{cm}$, where y_{cm} is the center-of-mass rapidity of colliding nuclei. In particular, this is the reason why the experimental distributions are multiplied y_{cm}. This representation is chosen in order to make different distributions of approximately the same width and the same height. This is convenient for comparison of shapes of these distributions. To make this comparison more quantitative, the data are fitted by a simple formula

$$\frac{dN}{dy} = a\left(\exp\left\{-(1/w_s)\cosh(y - y_{cm} - y_s)\right\} + \exp\left\{-(1/w_s)\cosh(y - y_{cm} + y_s)\right\}\right) \qquad (1)$$

where a, y_s and w_s are parameters of the fit. The form (1) is a sum of two thermal sources shifted by $\pm y_s$ from the midrapidity. The width w_s of the sources can be interpreted as $w_s = (\text{temperature})/(\text{transverse mass})$, if we assume that collective velocities in the sources have no spread with respect to the source rapidities $\pm y_s$. The parameters of the two sources are identical (up to the sign of y_s) because we consider only collisions of identical nuclei. Results of these fits are demonstrated in Fig. 1. Energy dependence of parameters y_s and w_s deduced from these fits revels no significant irregularities: they monotonously rise with the energy.

The above fit has been done by the least-squares method. Data were fitted in the rapidity range $|y - y_{cm}|/y_{cm} < 0.7$. The choice of this range is dictated by the data. As a rule, the data are available in this rapidity range, sometimes the data range is even more narrow ($40A$, $80A$ GeV and new data at $158A$ GeV [9]). We put the above restriction in order to treat different data in approximately the same rapidity range. Notice that the rapidity range should not be too wide in order to exclude contribution of cold spectators.

We met problems with fitting the data at $80A$ GeV [8] and the new data at $158A$ GeV [9]. These data do not go beyond the side maxima in the rapidity distributions. The fit within such a narrow region results in the source rapidities y_s very close (at $80A$ GeV) or even exceeding

*e-mail: Y.Ivanov@gsi.de

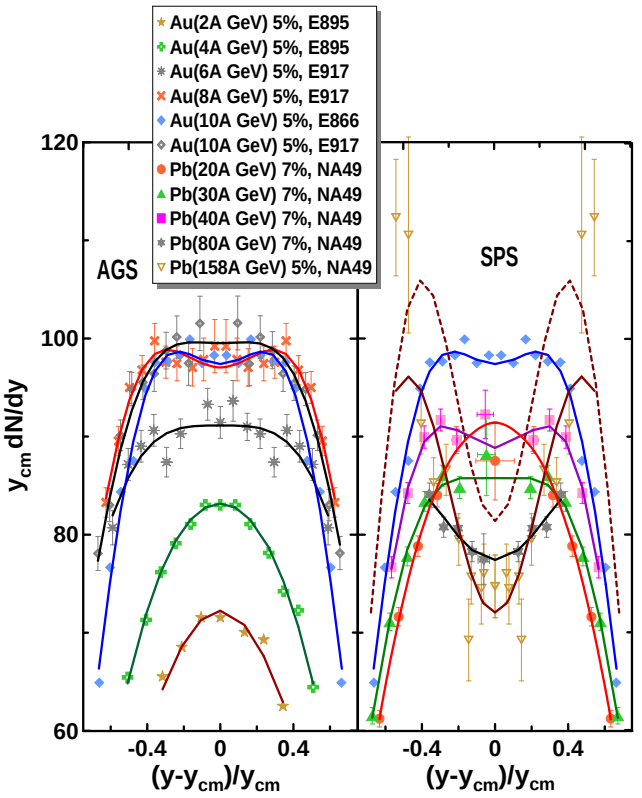

FIG. 1: Rapidity spectra of protons (for AGS energies) and net-protons ($p-\bar{p}$) (for SPS energies) from central collisions of Au+Au (AGS) and Pb+Pb (SPS). Experimental data are from collaborations E802 [1], E877 [2], E917 [3], E866 [4], and NA49 [5–9]. The percentage shows the fraction of the total reaction cross section, corresponding to experimental selection of central events. Solid lines connecting points represent the two-source fits by Eq. (1). The dashed line is the fit to old data on Pb(158A GeV)+Pb [5], these data themselves are not displayed.

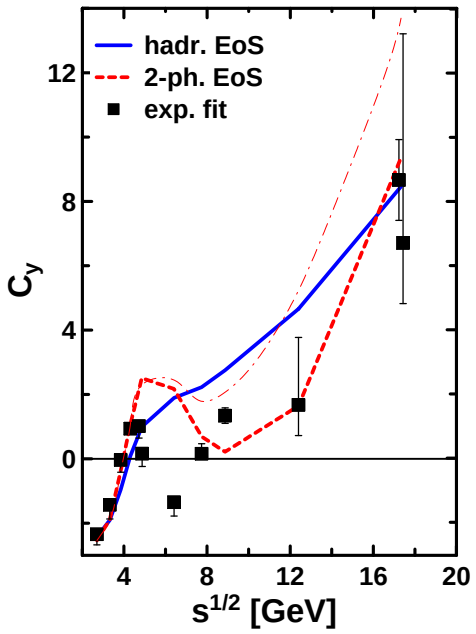

FIG. 2: Midrapidity reduced curvature of the (net)proton rapidity spectrum as a function of the center-of-mass energy of colliding nuclei as deduced from experimental data and predicted by 3FD calculations with hadronic EoS (hadr. EoS) [19] and a EoS involving a first-order phase transition into the quark-gluon phase (2-ph. EoS) [20]. The thin dashed-dotted line demonstrates the effect of the 2-ph. EoS without changing the friction in the quark-gluon phase.

(at 158A GeV) y_{cm} and a huge width w_s. As a result, the normalization of the net-proton rapidity distributions, as calculated with fit (1), turns out to be 330 (at 80A GeV) and 400 (at 158A GeV), which are considerably larger than the total proton number in colliding nuclei (=164). To avoid this problem, we performed a biased fit of these data. An additional condition restricted the total normalization of distribution (1) to be less than the total proton number in colliding nuclei (=164). This biased fit is the reason why the curve fitted to the new data at 158A GeV does not perfectly hit the experimental points. In particular, because of this problem we keep the old data at 158A GeV [5] in the analysis. We also use old data at 40A GeV, corresponding to centrality 7% [8], instead of recently published new data at higher (5%) centrality [9], since the data at the neighboring energies of 20A, 30A and 80A GeV are known only at centrality 7% [8]. Similarity of conditions, at which the data were taken, prevents excitation functions, which are of prime interest here, from revealing artificial irregularities.

Inspecting evolution of the spectrum shape with the incident energy rise, we observe an irregularity. Beginning from the lowest AGS energy to the top one the shape of the spectrum evolves from convex to slightly concave at 10A GeV. However, at 20A GeV the shape again becomes distinctly convex. With the further energy rise the shape again transforms from the convex form to a highly concave one. In order to quantify this trend, we introduce a reduced curvature of the spectrum in the midrapidity defined as follows

$$C_y \equiv \left(y_{cm}^3 \frac{d^3N}{dy^3}\right)_{y=y_{cm}} \Big/ \left(y_{cm}\frac{dN}{dy}\right)_{y=y_{cm}} = (y_{cm}/w_s)^2 \left(\sinh^2 y_s - w_s \cosh y_s\right). \quad (2)$$

This curvature is defined with respect to the "dimensionless" rapidity $(y-y_{cm})/y_{cm}$. The factor $1/\left(y_{cm}dN/dy\right)_{y=y_{cm}}$ is introduced in order to get rid of overall normalization of the spectrum, i.e. of the a parameter in terms of fit (1). The second part of Eq. (2) presents this curvature in terms of parameters of fit (1).

Values of the curvature C_y deduced from fit (1) to experimental data are displayed in Fig. 2. To evaluate errors of these deduced values, we estimated the errors produced by the least-squares method, as well as performed fits in different the rapidity ranges: $|y-y_{cm}|/y_{cm} < 0.5$ and $|y-y_{cm}|/y_{cm} < 0.9$, where it is appropriate, and also fits of the data at 80A GeV [8] and the new data at 158A

GeV [9] with different bias on the overall normalization of the distributions: $N_{\rm prot.} \leq 208$ (i.e., half of the net-nucleons can be participant protons) and $N_{\rm prot.} \leq 128$ (which is the hydrodynamic normalization of the distribution). The error bars present largest uncertainties among mentioned above. The lower point at $s^{1/2} = 17.3$ GeV corresponds to the new data at 158A GeV. Its upper error, as well as that of 80A-GeV point, results from the uncertainty of the normalization. The irregularity observed in Fig. 1 is distinctly seen here as a "zig-zag" irregularity in the energy dependence of C_y.

It is somewhat suspicious that the "zig-zag" irregularity happens at the border between the AGS and SPS energies. It could imply that this irregularity results from different ways of selecting central events in AGS and SPS experiments. However, there are indirect evidences of a physical (rather than methodical) nature of this irregularity. The difference between C_y values in two different experiments at 10A GeV can be taken as an estimate of the methodical uncertainty. The difference between C_y values at 10A GeV and 20A GeV is two to three times larger than this methodical uncertainty. Moreover, we could expect that C_y at 20A GeV would be larger than that at 10A GeV because the incident energy is higher and centrality selection at 20A GeV is less restrictive (7%) than at 10A GeV (5%). Contrary to these expectations the C_y at 20A GeV is smaller than that at 10A GeV. There should be a physical reason for that. Excitation functions of other quantities [21] deduced from the same AGS and SPS data do not reveal any misfit at the border between the AGS and SPS domains. The latter suggests that the AGS and SPS data were taken at similar physical conditions. However, new data taken at the same acceptance and the same centrality selection in this energy range are highly desirable to clarify this problem. Hopefully such data will come from new accelerators FAIR at GSI and NICA at Dubna, as well as from the low-energy-scan program at RHIC.

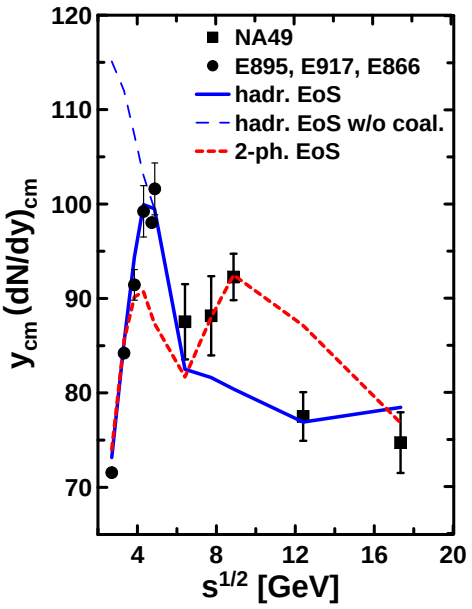

FIG. 3: Midrapidity value of the net-proton rapidity spectrum as a function of the center-of-mass energy of colliding nuclei. Experimental data are confronted to predictions of the 3FD model with the hadronic EoS (hadr. EoS) [19] and the EoS with a first-order phase transition (2-ph. EoS) [20]. The thin long-dashed line corresponds to the hadr.-EoS calculation without fragment production.

III. THREE-FLUID MODEL SIMULATIONS

Figure 2 also contains C_y deduced from results of 3FD simulations with a hadronic equation of state (hadr. EoS) [19] and a EoS involving a first-order phase transition into the quark-gluon phase (2-ph. EoS) [20]. To obtain y_s and w_s, the 3FD spectra were also fitted by the form (1). For central (5%) Au+Au collisions at AGS energies we performed our calculations taking a fixed impact parameter $b = 2$ fm; for the central (5%) Pb+Pb reaction at $E_{\rm lab} = 158A$ GeV, $b = 2.4$ fm which is the experimental estimate for this centrality [22]; for other central (7%) Pb+Pb collisions at 20A-80A GeV, $b = 3$ fm.

The 3FD model with the hadronic EoS reasonably reproduces a great body of experimental data in a wide energy range from AGS to SPS, see Ref. [17, 23–25]. Description of the rapidity distributions with the hadronic EoS is reported in Refs. [17, 18]. The reproduction of the distributions is quite good at the AGS energies and at the top SPS energies. At 40A GeV the description is still satisfactory. However, at 20A and 30A GeV the hadr.-EoS predictions completely disagree with the data, cf. [18]. At 20A GeV instead of a bump at the midrapidity the hadronic scenario predicts a quite pronounced dip. The problems with the description of the low-energy SPS data are clearly seen from Fig. 2 and also from Fig. 3, where midrapidity values of the rapidity distributions (multiplied by the center-of-mass rapidity) are presented. In Ref. [18] it was demonstrated that the problem with the low-energy SPS data can be solved by considerable softening the hadronic EoS. This softening may indicate an onset of the phase transition into the quark-gluon phase. Notice that a maximum in $y_{cm}(dN/dy)_{cm}$ at $s^{1/2} = 4.7$ GeV happens only because the light fragment production becomes negligible above this energy. The 3FD calculation without coalescence (i.e. without the fragment production) reveals a monotonous decrease of $y_{cm}(dN/dy)_{cm}$ beginning from $s^{1/2} = 2.7$ GeV, i.e. from the lowest energy considered here.

The 3FD simulations have been also done with a EoS involving a first-order phase transition into the quark-gluon phase (2-ph. EoS) [20]. In 2-ph. EoS the Gibbs construction was used for the mixed phase. These calculations well reproduce the AGS data up to the energy of

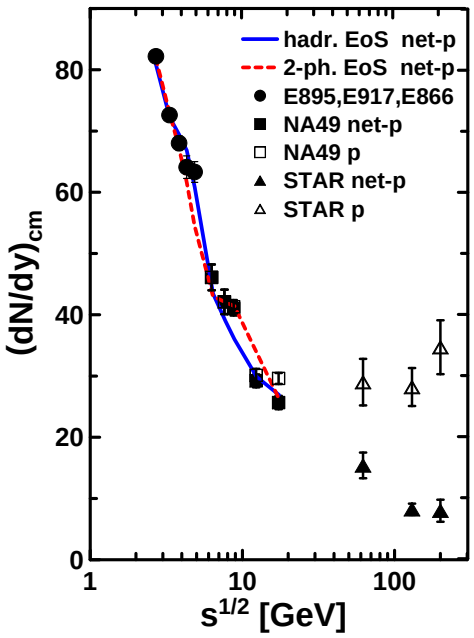

FIG. 4: The same as in Fig. 3 but in conventional representation (without multiplying by y_{cm}) and in a wider energy range including RHIC data on Au+Au collisions at 5% centrality [26]. Proton data [7, 26] are also displayed.

6A GeV, where the purely hadronic scenario is realized. The data at the top SPS energy are also reproduced, which is achieved by a proper tune of the inter-fluid friction in the quark-gluon phase. Quality of the reproduction of above data is approximately the same as that with the hadronic EoS, as it is, e.g., seen from Figs. 2 and from Fig. 3. However, at top AGS and lower SPS energies (8A-80A GeV), where the mixed phase turns out to be really important, the 2-ph. EoS completely fails. The fact that the 2-ph.-EoS line perfectly hits 20A-40A-GeV experimental points in Fig. 3 is just a coincidence, shapes of the distributions are completely wrong, as seen from Figs. 2. This failure cannot be cured by variations of neither the friction nor the freeze-out criterion.

However, the C_y curvature energy dependence in the first-order-transition scenario manifests qualitatively the same "zig-zag" irregularity (Fig. 2), as that in the data fit, while the hadronic scenario produces purely monotonous behaviour. This "zig-zag" irregularity of the first-order-transition scenario is also reflected in the midrapidity values of the (net)proton rapidity spectrum (Fig. 3). As for the experimental data, it is still difficult to judge if the "zig-zag" anomaly in the midrapidity values is statistically significant. In the conventional representation of the data (Fig. 4) without multiplying by y_{cm}, the irregularity of the $(dN/dy)_{cm}$ data is hardly visible. However, the conventional representation clearly demonstrates the overall trend of the data: the midrapidity net-proton yield gradually decreases with the incident energy, while the proton one stays approximately constant above the top SPS energy. Below the top SPS energy the proton and net-proton yields practically coincide. Model computations above the top SPS energy are at present not feasible because of high memory consumption required by the code (see discussion in Ref. [17]).

All above discussion concerns only central nuclear collisions. Experimental data on midcentral collisions is much less complete. The model calculations for midcentral collisions ($b \approx 6$ fm) reveal the same quantitative behaviour of the excitation functions of C_y and $(dN/dy)_{cm}$ both for hadr. EoS and 2-ph. EoS.

The baryon stopping depends on a character of interactions (e.g., cross sections) of the matter constituents. If during the interpenetration stage of colliding nuclei a phase transformation[1] of the hadronic matter into quark-gluonic one happens, one can expect a change of the stopping power of the matter at this time span. This is a natural consequence of a change of the constituent content of the matter because hadron-hadron cross sections differ from quark-quark, quark-gluon, etc. ones. This can naturally result in a non-monotonous behaviour of the shape of the (net)proton rapidity-spectrum at an incident energy, where onset of the phase transition occurs. Of course, the first-order transition does not happen abruptly. Within the Gibbs construction the fraction of the quark-gluon phase is gradually increasing, as well as weights of the corresponding cross sections. Therefore, a non-monotonous behaviour will show up only if the difference in cross sections in the hadronic and quark-gluon phases is large enough to override the above gradual increase of the fraction of the new phase. In fact, this is the case in the 3FD calculation with the phase transition (2-ph. EoS). The friction in the quark-gluon phase was tuned to reproduce the data at the top SPS energy. Naturally, it does not continuously match the friction in the hadronic phase. In terms of parton-parton cross sections, these cross sections in the quark-gluon phase turn out to be approximately twice as large as those in the hadronic phase[2]. In the quark-gluon phase these cross sections are compatible with those used, e.g., in a multiphase transport model [27] and a parton cascade model [28].

Notice that the proton rapidity distribution at 158A GeV is well described within the color-glass-condensate framework based on small-coupling QCD [29]. This mechanism drastically differs from that of hadronic stopping. Therefore, it is not surprising that the 3FD model requires very different (from the hadronic one) phenomenological friction at the 158A-GeV energy to reproduce the data.

[1] The term "phase transition" is deliberately avoided, since it usually implies thermal equilibrium.

[2] In the hadronic phase this parton cross section corresponds to the proton-proton one on the assumption of naive valence quark counting.

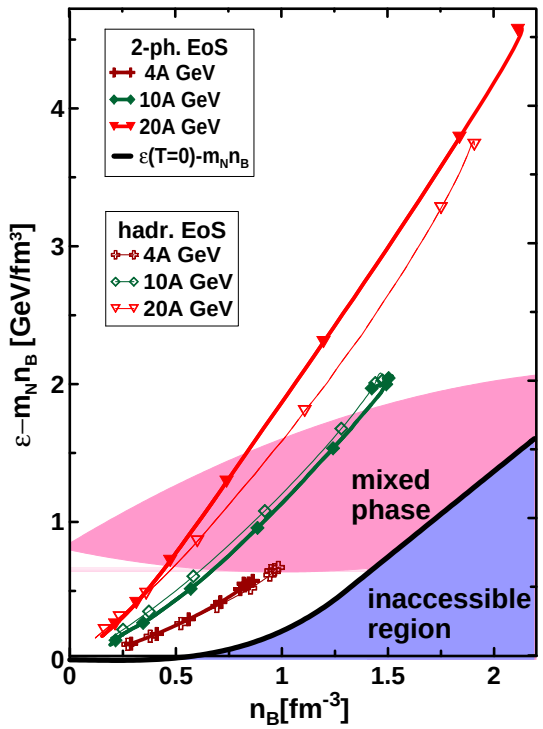

FIG. 5: Dynamical trajectories of the matter in the central box of the colliding nuclei (4fm×4fm×γ_{cm}4fm), where γ_{cm} is the Lorentz factor associated with the initial nuclear motion in the c.m. frame, for central ($b = 0$) collisions of Au+Au at $4A$ and $10A$ GeV energies and Pb+Pb at $20A$ GeV. The trajectories are plotted in terms of baryon density (n_B) and the energy density minus n_B multiplied by the nucleon mass ($\varepsilon - m_N n_B$). Only expansion stages of the evolution are displayed for two EoS's. Symbols on the trajectories indicate the time rate of the evolution: time span between marks is 1 fm/c.

However, if even the same friction is used in both phases, the calculated (with 2-ph. EoS) reduced curvature still reveals a "zig-zag" behaviour but with considerably smaller amplitude (see the thin dashed-dotted line in Fig. 2). This happens because the EoS in a generalized sense of this term, i.e. viewed as a partition of the total energy between kinetic and potential parts, also affects the stopping power. The friction is proportional to the relative velocity of the counter-streaming nuclei [17]. Therefore, it is more efficient when the kinetic-energy part of the total energy is higher, i.e. when the EoS is softer. This effect of the softening was demonstrated in Ref. [18]. It was shown that application of a soft, but still hadronic EoS changes the rapidity distributions, making them closer to the data at low SPS energies. This is precisely what the phase transition does: it makes the EoS essentially softer in the mixed-phase region. The latter naturally results in a non-monotonous evolution of the proton rapidity spectra with the energy rise.

Figure 5 demonstrates that the onset of the phase transition in the calculations indeed happens at top-AGS–low-SPS energies, where the "zig-zag" irregularity takes place. Similarly to that it has been done in Ref. [30], the figure displays dynamical trajectories of the matter in the central box placed around the origin $\mathbf{r} = (0, 0, 0)$ in the frame of equal velocities of colliding nuclei: $|x| \leq 2$ fm, $|y| \leq 2$ fm and $|z| \leq \gamma_{cm}$ 2 fm, where γ_{cm} is Lorentz factor associated with the initial nuclear motion in the c.m. frame. Initially, the colliding nuclei are placed symmetrically with respect to the origin $\mathbf{r} = (0, 0, 0)$, z is the direction of the beam. The ε-n_B representation is chosen because these densities are dynamical quantities and, therefore, are suitable to compare calculations with different EoS's. Subtraction of the $m_N n_B$ term is taken for the sake of suitable representation of the plot. Only expansion stages of the evolution are displayed, where the matter in the box is already thermally equilibrated. The size of the box was chosen to be large enough that the amount of matter in it can be representative to conclude on the onset of the phase transition and to be small enough to consider the matter in it as a homogeneous medium. Nevertheless, the matter in the box still amounts to a minor part of the total matter of colliding nuclei. Therefore, only the minor part of the total matter undergoes the phase transition at $10A$ GeV energy. As seen, the trajectories for two different EoS's are very similar at AGS energies and start to differ at SPS energies because of the effect of the phase transition.

IV. CONCLUSIONS

In conclusion, it is argued that the experimentally observed baryon stopping may indicate (within the present experimental uncertainties) a non-monotonous behaviour as a function of the incident energy of colliding nuclei. This reveals itself in a "zig-zag" irregularity in the excitation function of a midrapidity reduced curvature of the (net)proton rapidity spectrum. Notice that the energy location of this anomaly coincides with the previously observed anomalies for other hadron-production properties at the low SPS energies [21, 31]. The 3FD calculation with the hadronic EoS fails to reproduce this irregularity. At the same time, the same calculation with the EoS involving a first-order phase transition into the quark-gluon phase (within the Gibbs construction) [20] reproduces this "zig-zag" behaviour, however only qualitatively. Preliminary simulations with the EoS of Ref. [32], also based on the first-order phase transition but within the Maxwell construction, show the same qualitative trend. It is argued that the non-monotonous behaviour of the baryon stopping is a natural consequence of a phase transition. The question why these calculations do not qualitatively reproduce the "zig-zag" irregularity deserves special discussion elsewhere. It is very probable that either the Gibbs and Maxwell constructions are inappropriate for the fast dynamics of the heavy-ion collisions [33, 34] or the phase transition is not of the first order.

Fruitful discussions with B. Friman, M. Gazdzicki, J.

Knoll, P. Senger, H. Ströbele, V.D. Toneev and D.N. Voskresensky are gratefully acknowledged. I am grateful to A.S.Khvorostukhin, V.V.Skokov, and V.D.Toneev for providing me with the tabulated 2-ph. EoS. I am grateful to members of the NA49 Collaboration for providing me with the experimental data in the digital form. This work was supported in part by the Deutsche Bundesministerium für Bildung und Forschung (BMBF project RUS 08/038), the Deutsche Forschungsgemeinschaft (DFG projects 436 RUS 113/558/0-3 and WA 431/8-1), the Russian Foundation for Basic Research (RFBR grant 09-02-91331 NNIO_a), and the Russian Ministry of Science and Education (grant NS-7235.2010.2).

[1] L. Ahle *et al.* (E802 Collab.), Phys. Rev. C **60**, 064901 (1999).
[2] J. Barrette *et al.* (E877 Collab.), Phys. Rev. C **62**, 024901 (2000).
[3] B.B. Back et al., (E917 Collab.), Phys. Rev. Lett. **86** , 1970 (2001).
[4] J. Stachel, Nucl. Phys. **A654**, 119c (1999).
[5] H. Appelshäuser *et al.* (NA49 Collab.), Phys. Rev. Lett. **82**, 2471 (1999).
[6] T. Anticic *et al.* (NA49 Collab.), Phys. Rev. C **69**, 024902 (2004).
[7] C. Alt *et al.* (NA49 Collab.), Phys. Rev. C **73**, 044910 (2006).
[8] C. Blume (NA49 Collab.), J. Phys. **G34**, S951 (2007).
[9] H. Strobele (NA49 Collab.), e-Print: arXiv:0908.2777 [nucl-ex].
[10] W. Cassing and E.L. Bratkovskaya, e-Print: arXiv:0907.5331 [nucl-th].
[11] J. Steinheimer *et al.*, e-Print: arXiv:0905.3099 [hep-ph]
[12] E.L. Bratkovskaya, M. Bleicher, M. Reiter, S. Soff, H. Stoecker, M. van Leeuwen, S.A. Bass, and W. Cassing, Phys. Rev. C **69**, 054907 (2004).
[13] H. Weber, E.L. Bratkovskaya, W. Cassing, and H. Stöcker, Phys. Rev. C **67**, 014904 (2003).
[14] H. Weber, E.L. Bratkovskaya, and H. Stoecker, Phys. Rev. C **66**, 054903 (2002).
[15] A.B. Larionov, O. Buss, K. Gallmeister, and U. Mosel, Phys. Rev. C **76**, 044909 (2007).
[16] M. Wagner, A.B. Larionov, and U. Mosel, Phys. Rev. C **71**, 034910 (2005).
[17] Yu.B. Ivanov, V.N. Russkikh, and V.D. Toneev, Phys. Rev. C **73**, 044904 (2006).
[18] Yu.B. Ivanov and V.N. Russkikh, PoS(CPOD07)008 (2007), arXiv:0710.3708 [nucl-th].
[19] V.M. Galitsky and I.N. Mishustin, Sov. J. Nucl. Phys. **29**, 181 (1979).
[20] A.S.Khvorostukhin, V.V.Skokov, K.Redlich, and V.D.Toneev, Eur. Phys. J. **C48**, 531 (2006).
[21] C. Alt *et al.* [NA49 Collab.], Phys. Rev. C **77**, 024903 (2008).
[22] C. Alt *et al.* (NA49 Collab.), Phys. Rev. C **68**, 034903 (2003).
[23] V.N. Russkikh and Yu.B. Ivanov, Phys. Rev. C **74** (2006) 034904.
[24] Yu.B. Ivanov and V.N. Russkikh, Eur. Phys. J. **A 37**, 139 (2008); Phys. Rev. C **78**, 064902 (2008).
[25] Yu.B. Ivanov, I.N. Mishustin, V.N. Russkikh, and L.M. Satarov, Phys. Rev. C **80**, 064904 (2009).
[26] B.I. Abelev *et al.* [STAR Collab.], Phys. Rev. C **79**, 034909 (2009).
[27] Bin Zhang, Lie-Wen Chen, and Che Ming Ko, J. Phys. **G 35**, 065103 (2008).
[28] Zhe Xu and C. Greiner, Phys. Rev. C **76**, 024911 (2007).
[29] Y. Mehtar-Tani and G. Wolschin, Phys. Rev. Lett. **102**, 182301 (2009); Phys. Rev. C **80**, 054905 (2009).
[30] I.C. Arsene, *et al.*, Phys. Rev. C **75**, 034902 (2007).
[31] M. Gazdzicki and M. I. Gorenstein, Acta Phys. Polon. B **30**, 2705 (1999).
[32] L.M. Satarov, M.N. Dmitriev, and I.N. Mishustin, Yad. Fiz. **72**, 1444 (2009) [Phys. Atom. Nucl. **72**, 1390 (2009)].
[33] J. Randrup, Phys. Rev. C **79**, 054911 (2009).
[34] V.V. Skokov and D.N. Voskresensky, JETP Lett. **90**, 223 (2009); Nucl. Phys. **A828**, 401 (2009).